

A New Low-Light Image Enhancement Algorithm using Camera Response Model *

Zhenqiang Ying, Ge Li, Yurui Ren, Ronggang Wang, and Wenmin Wang
SECE, Shenzhen Graduate School
Peking University
Shenzhen, China

{zqying, yrren}@pku.edu.cn, geli@ece.pku.edu.cn, rgwang@pkusz.edu.cn, wangwm@ece.pku.edu.cn

Abstract

Low-light images are not conducive to human observation and computer vision algorithms due to their low visibility. To solve this problem, many image enhancement techniques have been proposed. However, existing techniques inevitably introduce color and lightness distortion when increasing visibility. To lower the distortion, we propose a novel enhancement method using the response characteristics of cameras. First, we investigate the relationship between two images with different exposures to obtain an accurate camera response model. Then we borrow the illumination estimation techniques to estimate the exposure ratio map. Finally, we use our camera response model to adjust each pixel to its desired exposure according to the estimated exposure ratio map. Experiments show that our method can obtain enhancement results with less color and lightness distortion compared to several state-of-the-art methods.

1. Introduction

Computer vision and multimedia algorithms require high-visibility input images [16]. However, images taken in low-light condition are often of low visibility. Therefore, we need to enhance those images before further processing. In general, image enhancement techniques can make the input images look better and be more suitable for specific algorithms [38, 17]. Existing image enhancement techniques can be divided into two major categories: global enhancement [35, 17, 28, 6, 30, 1, 29, 9, 32, 3] and local enhancement [36, 12, 16, 38, 34, 37].

Global enhancement performs same processing on all image pixels regardless of their spatial distribution. Lin-

ear amplifying is a simple and straightforward global enhancement method. However, bright regions might be saturated and result in detail loss. To avoid the problem, some image enhancement methods adopt non-linear monotonic functions (e.g. power-law [4], logarithm [26] and gamma function [13]) to perform enhancements. As another way to avoid saturation, histogram equalization (HE) [18] can improve the contrast effectively and became a widely-used technique. Many extensions of HE are proposed to take some restrictions into account such as brightness preservation [17, 35, 7] and contrast limitation [28]. However, global enhancement may results in detail loss in some local areas because a global processing can not ensure all local areas be well enhanced.

Taking the spatial distribution of pixels into consideration, local enhancement can obtain better results and become the main-stream of recent techniques. Local histogram equalization [31, 2] adopt the sliding window strategy to perform HE locally. Based on the observation that the inverted low-light images are closed to hazy images, dehazing techniques are borrowed to solve low-light image enhancement in [11, 19]. However, the basic models of above methods are lacking in physical explanation [16]. To provide a physical meaningful model for image enhancement, Retinex theory assumes that the amount of light reaching observers can be decomposed into two parts: illumination and scene reflection. Most Retinex-based methods get enhanced results by removing the illumination part [36] while the others [12, 38, 16] keep a portion of the illumination to preserve naturalness. However, those methods may suffer from over- and under- enhancement due to ignoring the camera response characteristics.

To preserve the image naturalness and achieve more accurate enhancement results, in-camera processing needs to be considered when designing enhancement algorithms. For most digital cameras, the pixel value is not directly proportional to the irradiance that fall on the camera [5].

*This work was supported by the grant of National Science Foundation of China (No.U1611461), Shenzhen Peacock Plan (20130408183003656), and Science and Technology Planning Project of Guangdong Province, China (No. 2014B090910001 and No. 2014B010117007).

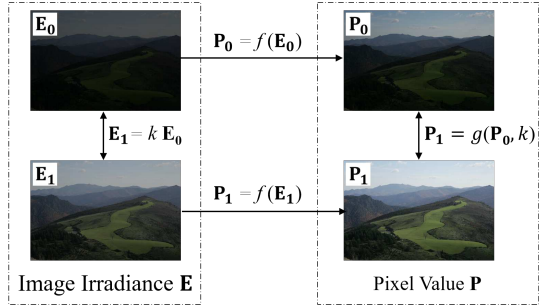


Figure 1. The Image irradiance and pixel value of two images captured in the same scene with different exposures.

The nonlinear function relating camera sensor irradiance and image pixel value is called camera response function (CRF). In this paper, we provide a new enhancement algorithm taking the CRF into consideration. Specifically, first we present our enhancement framework which consists of two key problems: one is to find a suitable camera response model and the other is to determine the exposure ratio map. From the observation on histogram characteristics of two images that only differ in exposure, we then provide an accurate camera response model allowing us to adjust the exposure of the input image. Next, we estimate the exposure ratio map with the help of illumination estimation techniques. Finally, we propose our enhancement algorithm based on the camera response model and the estimated exposure ratio map. Experimental results show that our model can reduce the mean RMSE by an order of magnitude compared to that of other existing two-parameter models. Besides, the proposed method can enhance images with less color and lightness distortion compared to several state-of-the-art methods.

2. Background

In general, camera manufacturers use some nonlinear in-camera processes such as white balance, demosaicking to improve the visual quality of captured images. As shown in Fig. 1, those nonlinear processes can be modeled as:

$$\mathbf{P} = f(\mathbf{E}), \quad (1)$$

where \mathbf{E} is the image irradiance, \mathbf{P} is the pixel value and f is the nonlinear function CRF. To figure out the common characteristics of f , three assumptions are made [14]. First, f is the same for all pixels on the sensor. Second, the range of $f(\cdot)$ can be normalized to $[0, 1]$. Third, f monotonically increases. Under these assumptions, define $\mathcal{F} : [0, 1] \rightarrow [0, 1]$ as the theoretical space of f :

$$\mathcal{F} := \{f | f(0) = 0, f(1) = 1, x > y \Leftrightarrow f(x) > f(y)\}. \quad (2)$$

Given \mathcal{F} , many methods have been developed to estimate (or reconstruct) f . Without assuming its functional form,

f can be obtained from a set of images taken at different exposures for a given scene. However, the functional form of f is needed to build a camera response model for low-light image enhancement problem.

The functional form of f can be estimated directly by assuming an approximation model (e.g. polynomial [23] and trigonometric [15]) and then find the best model parameters based on some optimization criterion [14, 10, 24]. To improve the model accuracy, an empirical model called EMoR is proposed in [14] by performing Principle Component Analysis on DoRF database that contains 201 real-world response curves. However, empirical models lack the differentiable property of an analytic model. To avoid this problem, Ng *et al.* presented generalized gamma curve model (GCCM) to estimate f [25].

The functional form of f can also be estimated indirectly by modeling the brightness transform function (BTF). As shown in Fig. 1, BTF is the mapping function between two images \mathbf{P}_0 and \mathbf{P}_1 captured in the same scene with different exposures:

$$\mathbf{P}_1 = g(\mathbf{P}_0, k), \quad (3)$$

where g is the BTF and k is the exposure ratio. Then, the CRF can be obtained by solving the following comparative equation:

$$g(f(\mathbf{E}), k) = f(k\mathbf{E}), \quad (4)$$

Many BTF models have been proposed. Commonly used Gamma Correction cannot obtain realistic enhancement results due to the presumption of an unreasonable CRF which does not pass the origin. Affine Correction is preferable to Gamma Correction because of the implicit form of f passing the origin. Preferred Correction outperforms the two correction methods above since it has a parameter to control the softness of the transition into toe and shoulder regions of the response function rather than hard clipping [22].

3. Our Approach

A low-light image may either be globally under-exposed or locally under-exposed, so we cannot get all pixels well-exposed using an uniform exposure ratio k . In order to solve general low-light image enhancement, we extend k in Eq. 3 to a matrix as

$$\mathbf{P}' = g(\mathbf{P}, \mathbf{K}). \quad (5)$$

where \mathbf{P} and \mathbf{P}' are the input image and the desired output image respectively. Unlike the uniform exposure ratio in Eq. 3, \mathbf{K} is an exposure ratio map indicating the desired exposure ratio for each pixel. Based on our definition, the low-light enhancement problem can be transformed into the estimate of g and \mathbf{K} . This section is organized as follows: In Sect. 3.1, we introduce our enhancement framework combining the camera response model and traditional Retinex model. In Sect. 3.2, our camera response model is proposed to solve g . In Sect. 3.3, the estimation of \mathbf{K} is presented.

3.1. Framework

Traditional Retinex model assumes that the amount of light reaching observers can be decomposed into two parts as follows:

$$\mathbf{E} = \mathbf{R} \circ \mathbf{T}, \quad (6)$$

where \mathbf{R} and \mathbf{T} are the scene reflectance map and the illumination map, respectively. The operator \circ represents element-wise multiplication and \mathbf{E} is the light reaching camera, *i.e.* the image irradiance. Existing Retinex-based methods simply take \mathbf{E} as the input image and \mathbf{R} as the desired output. As aforementioned, in most cameras, there exists a nonlinear radiometric response function f . Therefore, f should be considered in forming the actual input image \mathbf{P} and the desired recovery image \mathbf{P}' :

$$\mathbf{P} = f(\mathbf{E}), \quad \mathbf{P}' = f(\mathbf{R}). \quad (7)$$

The desired recovery can be written as:

$$\begin{aligned} \mathbf{P}' &= f(\mathbf{R}) \stackrel{\text{Eq. 6}}{=} f(\mathbf{E} \circ (\mathbf{1} \oslash \mathbf{T})) \\ &\stackrel{\text{Eq. 4}}{=} g(f(\mathbf{E}), \mathbf{1} \oslash \mathbf{T}) = g(\mathbf{P}, \mathbf{1} \oslash \mathbf{T}) \end{aligned} \quad (8)$$

where \oslash represents element-wise division. From Eq. 5 and Eq. 8, we can find the relation between \mathbf{T} and \mathbf{K} :

$$\mathbf{K} = \mathbf{1} \oslash \mathbf{T}. \quad (9)$$

The result is physically meaningful: to reach the desired exposure, the dark areas of the image should be assigned a large exposure ratio while the bright areas should be assigned a small exposure ratio.

Based on the Retinex theory, we show that the exposure ratio map \mathbf{K} can be obtained by estimating the illumination map \mathbf{T} . As a result, many techniques from Retinex-based methods can be migrated to our enhancement framework. Our framework is easy to extend by borrowing different Retinex decomposition techniques or camera models.

3.2. Camera Response Model

A camera response model consists of two parts: CRF model and BTF model. The parameters of CRF model is determined only by camera while that of BTF model is determined by camera and exposure ratio. In this subsection, we first propose our BTF model based on the observation of two different exposure images. Then we derive the corresponding CRF model by solving the comparometric equation. Finally, we discuss how to determine the model parameters and present the final form of g .

3.2.1 BTF Estimation

To estimate the BTF g , we select a pair of images \mathbf{P}_0 and \mathbf{P}_1 that differ only in exposure. Then we plot their histograms

of each color channel, as shown in Fig. 2. Noticing that the histograms of the under-exposed image mainly concentrate in low-brightness area, if we perform linear amplification of pixel values before traditional gamma correction, then the resulting image will be very close to the real well-exposed image. Therefore, we can use a two-parameter function to describe the BTF model as

$$\mathbf{P}_1 = g(\mathbf{P}_0, k) = \beta \mathbf{P}_0^\gamma, \quad (10)$$

where β and γ are parameters in our BTF model related to exposure ratio k . The observation also shows that different color channels have approximately same model parameters. The underlying reason is that the response curves of different color channels are approximately identical for general cameras.

3.2.2 CRF Estimation

In our BTF model, β and γ are determined by the camera parameters and exposure ratio k . To find their relationship, we need to obtain the corresponding CRF model. The CRF model can be derived by solving the following comparometric equation (plug $g = \beta f^\gamma$ to Eq. 4):

$$f(kE) = \beta f(E)^\gamma. \quad (11)$$

The closed-form solution of f is provided in [22] as follows:

$$f(E) = \begin{cases} e^{b(1-E^a)}, & \text{if } \gamma \neq 1, \\ E^c, & \text{if } \gamma = 1. \end{cases} \quad (12)$$

where a and b are model parameters in the case of $\gamma \neq 1$:

$$a = \log_k \gamma, \quad b = \frac{\ln \beta}{1 - \gamma}; \quad (13)$$

And c is model parameter in the case of $\gamma = 1$:

$$c = \log_k \beta. \quad (14)$$

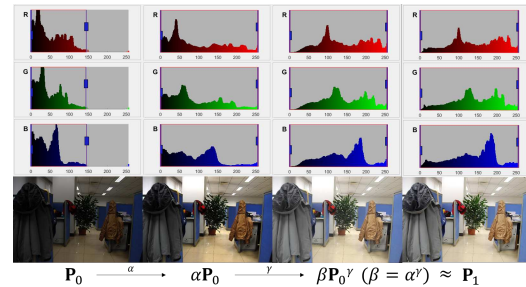


Figure 2. Observation. From left to right: An under-exposure image \mathbf{P}_0 , apply multiplication $\alpha \mathbf{P}_0$, apply gamma function $(\alpha \mathbf{P}_0)^\gamma$ and the well-exposure image \mathbf{P}_1 under the same scene. The histograms of red, green and blue color channels are plotted above the corresponding image respectively.

Two CRF models can be derived from two cases of Eq. 12. When $\gamma = 1$, the CRF model is a power function and the BTF model is a simple linear function. As some camera manufacturers design f to be a gamma curve, it can fit these cameras perfectly. When $\gamma \neq 1$, the CRF model is a two-parameter function and the BTF model is a non-linear function. Since the BTF is non-linear for most cameras, we mainly consider the case of $\gamma \neq 1$.

To evaluate the accuracy of the two CRF models, we perform least square fit of the camera response models to the 201 real-world camera response curves in the DoRF database. The goodness of fit for each curve is measured by Root Mean Square Error (RMSE). As shown in Table 1, our model performs the best in single parameter models when $\gamma = 1$ and performs the best among the two-parameter models when $\gamma \neq 1$. Besides, the RMSE of our model ($\gamma \neq 1$) is an order of magnitude smaller than that of other two-parameter models. Note that although the closed form of our model is provided in [22], the model has not been used in the field of image enhancement.

3.2.3 Model Parameter Determination

From Eq. 13, the parameters in our BTF model can be derived as

$$\beta = e^{b(1-k^a)}, \quad \gamma = k^a. \quad (15)$$

Since the camera response curve is fixed for a specific camera, the parameters of CRF (a and b) can be obtained by fitting the curve. Based on the model, given an input image \mathbf{P}_0 and arbitrary exposure ratio k_* , we can obtain the corresponding image \mathbf{P}_* that differ only in exposure from our BTF model:

$$g(\mathbf{P}_0, k_*) = \mathbf{P}_* = \beta_* \mathbf{P}_0^{\gamma_*} = e^{b(1-k_*^a)} \mathbf{P}_0^{(k_*^a)}. \quad (16)$$

3.3. Exposure Ratio Map Estimation

Since \mathbf{K} is inversely proportional to illumination map \mathbf{T} , we can estimate \mathbf{T} first and then solve \mathbf{K} . Many illu-

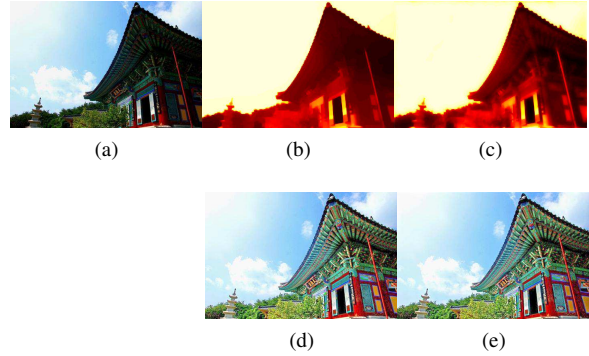


Figure 3. (a) Input image. (b) Estimated illumination map by [16] (0.21s). (c) Our illumination map (0.15s). (d) Enhanced result using (b). (e) Enhanced result using (c).

mination estimation methods have been proposed for image enhancement task. We employ the sped-up solver in [16] with a small modification on the design of weight matrix to make it faster. As in [16], we adopt the lightness component as the initial estimation of illumination:

$$\mathbf{L}(x) = \max_{c \in \{R, G, B\}} \mathbf{P}_c(x) \quad (17)$$

for each individual pixel x . Unlike in [16], we design the weight matrix as

$$\mathbf{W}_d(x) = \frac{1}{|\sum_{y \in \omega(x)} \nabla_d \mathbf{L}(y)| + \epsilon}, \quad d \in \{h, v\}, \quad (18)$$

where $|\cdot|$ is the absolute value operator, $\omega(x)$ is the local window centered at the pixel x and ϵ is a very small constant to avoid the zero denominator. The first order derivative filter ∇_d contains ∇_h (horizontal) and ∇_v (vertical). The refined illumination map \mathbf{T} is solved by optimization:

$$\min_{\mathbf{T}} \sum_x \left((\mathbf{T}(x) - \mathbf{L}(x))^2 + \lambda \sum_{d \in \{h, v\}} \frac{\mathbf{W}_d(x) (\nabla_d \mathbf{T}(x))^2}{|\nabla_d \mathbf{L}(x)| + \epsilon} \right), \quad (19)$$

where λ is the coefficient to balance the involved two terms. Since the problem now only involves quadratic terms, the closed-form solution is available. Therefore, the result can be directly computed without requiring any iterations. Although the illumination map in [16] is sharper than that by the modified version, the efficiency is greatly improved and the two enhanced results show no significant visual difference, as shown in Fig. 3.

The estimated exposure ratio map \mathbf{K} can be obtained using \mathbf{T} via Eq. 9. To prevent the exposure ratio becomes infinite when the illumination tends to zero, we set the lower bound of the illumination:

$$\mathbf{K}(x) = \frac{1}{\max(\mathbf{T}(x), \epsilon)}. \quad (20)$$

Table 1. Compared with existing CRF models.

Mean RMSE ($\times 10^{-2}$) of Various CRF models				
Model	Number of model parameters			
	1	2	3	4
polynomial	7.37	3.29	1.71	1.06
trigonometric	6.83	3.91	2.58	1.89
GGCM f	5.18	2.34	1.16	0.60
GGCM g	8.17	1.46	0.97	0.49
EMOR	4.00	1.73	0.63	0.25
Gamma Correction	41.82	N.A.	N.A.	N.A.
Zeta Correction	N.A.	4.15	N.A.	N.A.
Preferred Correction	N.A.	N.A.	1.00	N.A.
Ours ($\gamma = 1$)	3.46	N.A.	N.A.	N.A.
Ours ($\gamma \neq 1$)	N.A.	0.90	N.A.	N.A.

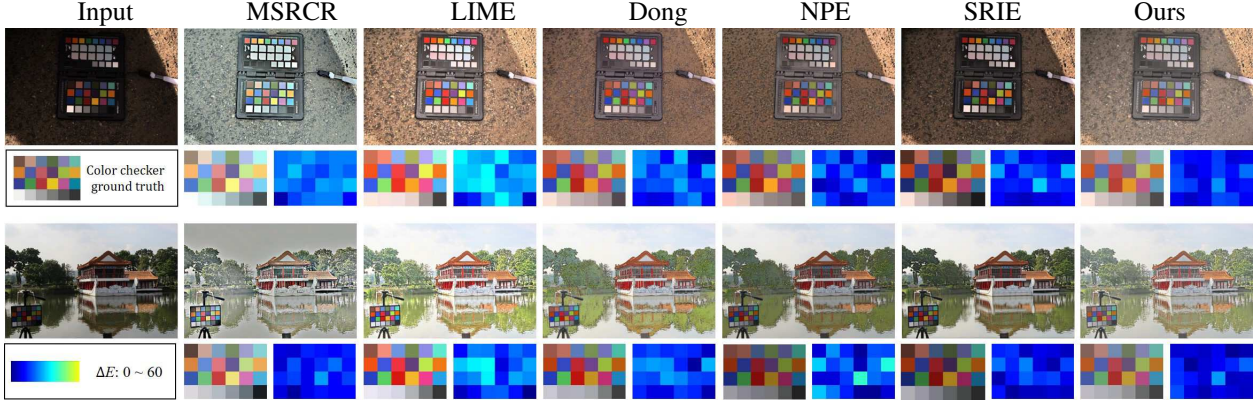


Figure 4. Examples of color distortion visualization. The odd rows show the original image and the results of various enhancement methods, and the even rows show the extracted color checker and the color distortion visualization of each method.

Finally, based on our camera response model and the estimated exposure ratio map, we can enhance each pixel $\mathbf{P}(x)$ of the low-light input image as

$$\mathbf{P}'_c(x) = e^{b(1-\mathbf{K}(x)^a)} \mathbf{P}_c(x)^{\mathbf{K}(x)^a}. \quad (21)$$

4. Experiments

In this section, we design several experiments to qualitatively analyze the performance of our enhancement algorithm. We compare our algorithm with several state-of-the-art methods: MSRCR [27], LIME [16], Dong [11] NPE [38] and SRIE [20]. In order to maintain the fairness of the comparison, all the codes are in Matlab and all the experiments are conducted on a PC running Windows 10 OS with 64G RAM and 3.4GHz CPU. The parameters of our enhancement algorithm are fixed in all experiments: $\lambda = 1$, $\epsilon = 0.001$, and the size of local window $\omega(x)$ is 5. Besides, we assume that no information about the camera is provided and use a fixed camera parameters ($a = -0.3293$, $b = 1.1258$) that can fit most cameras. The most time-consuming part of our algorithm is illumination map optimization. We employ the multi-resolution preconditioned conjugate gradient solver ($O(N)$) to solve it efficiently.

4.1. Color Distortion Evaluation

Several state-of-the-art methods are evaluated on two public Color Checker datasets (UEA [20] and NUS [8])

Table 2. Color Distortion (Mean ΔE).

Method	UEA	NUS
MSRCR	25.93	21.04
Dong	20.53	23.56
NPE	19.68	19.91
LIME	25.20	28.89
SRIE	22.71	19.31
<i>Ours</i>	16.99	17.75

Table 3. Quantitative measurement results of lightness distortion (LOE).

Method	UEA	NUS	VV	LIME	NPE	MEF
MSRCR	1677	3043	2728	1836	1890	1686
Dong	1337	771	853	1244	1012	1065
NPE	691	413	821	1471	646	1158
LIME	957	1434	1275	1324	1120	1079
SRIE	657	413	551	824	533	754
<i>Ours</i>	501	613	431	499	506	345

to measure the color distortion of enhanced results. The images in these datasets are captured with a color checker board in the scene to provide a color reference. Fig. 4 shows two example images in the dataset and their enhanced result by different algorithms. To measure the color distortion, we adopt ΔE as in [39]. The color difference ΔE is defined as the Euclidean distance between two colors in CIE Lab color space:

$$\Delta E = \sqrt{(L_1 - L_2)^2 + (a_1 - a_2)^2 + (b_1 - b_2)^2} \quad (22)$$

where L_* , a_* and b_* are three components of CIE Lab color space. Specifically, we first calculate the average RGB values in each color patch of the enhanced images. Then we map these pixel value to Lab space and calculate the ΔE color difference with standard color. The overall color distortion for an image is estimated as the average ΔE color difference of 24 colors in color checker board. Finally, we calculate the color distortion of all images in each datasets and obtain the mean color distortion. As shown in Table 2, our method achieves the smallest color distortion under both datasets.

4.2. Lightness Distortion Evaluation

To evaluate the performance of our method, we performed our methods with the several state-of-art methods on hundreds of low-light images from several public datasets:

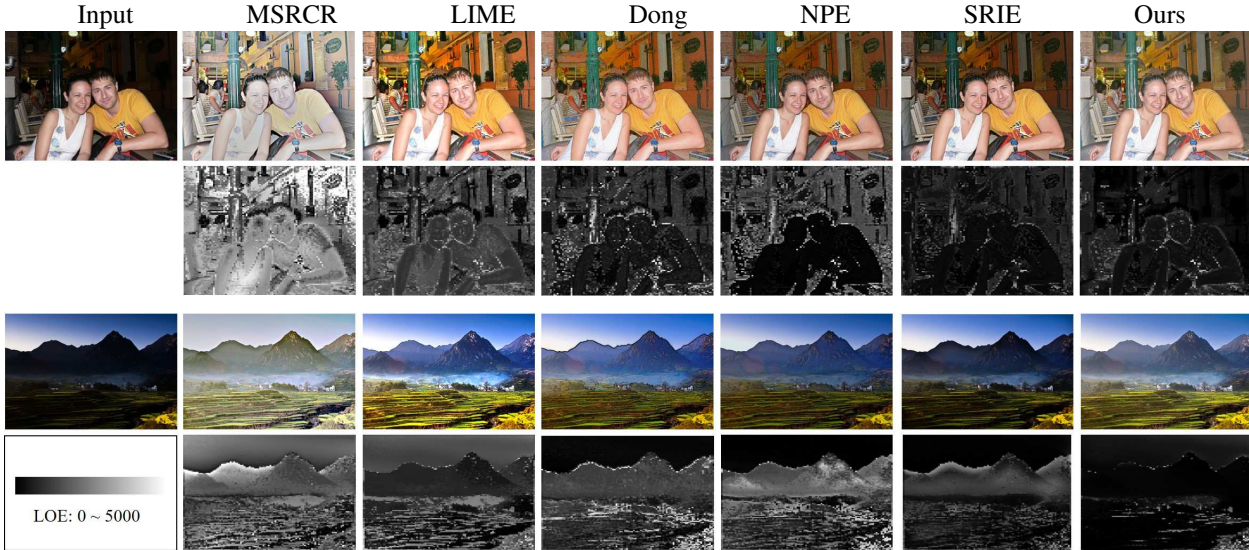


Figure 5. Examples of lightness distortion visualization. The odd rows show the original image and the results of various enhancement methods, and the even rows show the visualization of each method’s lightness distortion (RD).

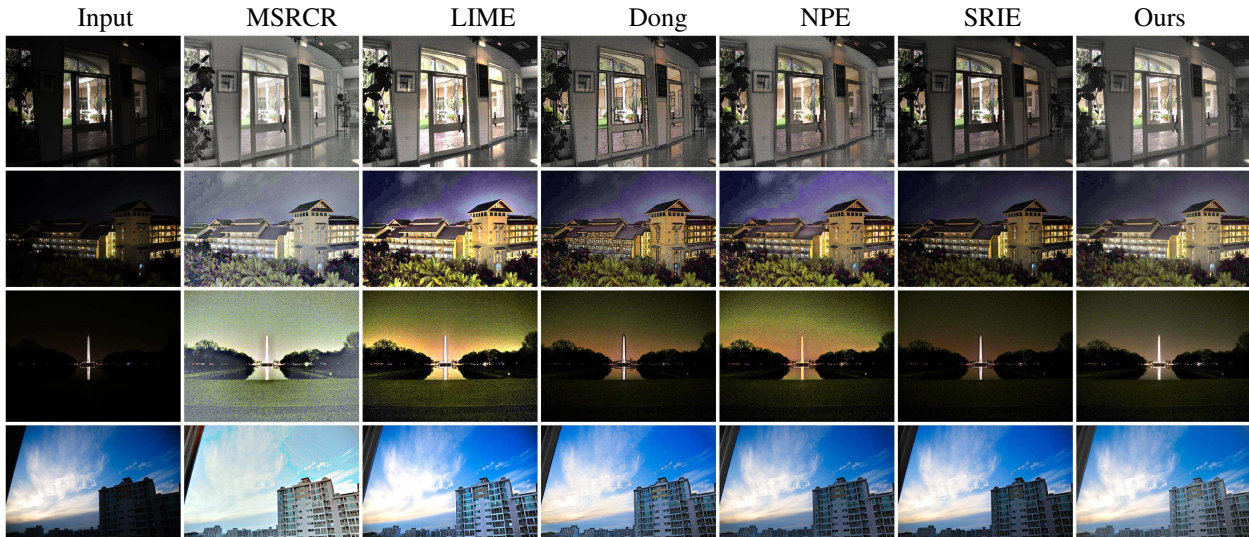


Figure 6. Visual comparison among the competitors on different scenes.

VV [33], LIME [16], NPE [38], and MEF [21]. MEF is a multi-exposure dataset, we select a low-light image from each multi-exposure set for evaluation.

We use lightness order error (LOE) to objectively measure the lightness distortion of enhanced results. LOE is defined as

$$LOE = \frac{1}{m} \sum_{x=1}^m RD(x) \quad (23)$$

where $RD(x)$ is the relative order difference of the lightness between the original image P and its enhanced version

P' for pixel x , which is defined as follows:

$$RD(x) = \sum_{y=1}^m U(\mathbf{L}(x), \mathbf{L}(y)) \oplus U(\mathbf{L}'(x), \mathbf{L}'(y)), \quad (24)$$

where m is the pixel number, \oplus stands for the exclusive-or operator, $\mathbf{L}(x)$ and $\mathbf{L}'(x)$ are the maximum values among three color channels at location x of the input images and the enhanced images, respectively. The function $U(p, q)$ returns 1 if $p \geq q$, 0 otherwise.

As suggested in [16, 38], down-sampling is needed to reduce the complexity of computing LOE. We down-sample all images to 100×100 when evaluating LOE. As shown in Table 3, our algorithm outperforms the others in almost

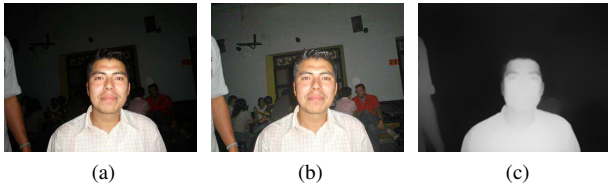


Figure 7. An example of a failure case. (a) Raw image. (b) Enhanced result. (c) Estimated illumination T .

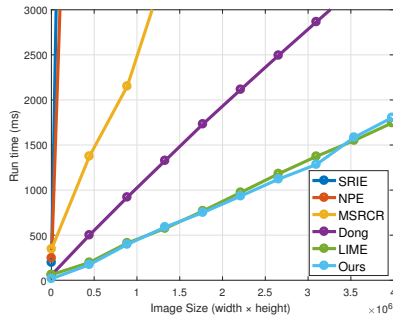


Figure 8. Time comparison among different methods with varying image sizes

all datasets. This means that our algorithm can maintain the naturalness of images well. We also provide a visualization of lightness distortion on two cases in Fig. 5, from which, we can find our results have the smallest lightness distortion. The results of MSRCR lose the global lightness order and suffer from severe lightness distortion. Although the results of LIME is visually pleasant, they are full of lightness distortion. The results of Dong, NPE and SRIE can only retain the lightness order in the well-exposed area. Fig. 6 shows more examples for visual comparison.

4.3. Time Cost

Fig. 8 gives the comparison among different methods in terms of time cost. Although SRIE and NPE produce small distortion, they are quite time-consuming. Dong, LIME and our method are linear time solvers and Dong is about 2 times slower than the others. Our method achieves smaller distortion than LIME with the similar time cost.

4.4. Limitation And Future Work

Fig. 7 shows an example of a failure case of our technique that the hair of the man turns to be grey because of over-enhancement. This is due to the dark area behind his head blending with his black hair. As shown in Fig. 7 (c), the hair is mistaken as the dark background in the estimated illumination map and therefore is enhanced along with the background. Such mistake is a result of the existing illumination map estimation techniques. This highlights a direction for future work. To avoid the over-enhancement due to the ignorance of the scene content, semantic understanding

is required. With further refinement, we might employ the deep learning techniques to estimate the illumination map.

Though we assume a fixed camera parameters for all experiments, how using the camera-specific parameters alters performance has not yet been analyzed. For future work, we intend to explore if it is necessary and practical to use single image CRF estimation techniques to obtain the accurate CRF.

5. Conclusion

In this paper, we propose an efficient naturalness preserved method to enhance low-light images. First, we propose our enhancement framework combining the camera response model and traditional Retinex model. Second, based on our framework, we solve two problems: 1) we propose an accurate camera response model that can reduce the mean RMSE by an order of magnitude compared to that of other existing two-parameter models; 2) we present a fast solution to the exposure map estimation. Third, we propose an image enhancement algorithm using our camera response model and estimated exposure map. The experimental results have revealed the advance of our method compared with several state-of-the-art alternatives. Moreover, our method is general to different camera response model as well as different exposure map estimation strategies. To encourage future works and allow more experimental verification and comparisons, we make the source code open. More testing results can be found on our project website¹.

References

- [1] M. Abdullah-Al-Wadud, M. H. Kabir, M. A. A. Dewan, and O. Chae. A dynamic histogram equalization for image contrast enhancement. *IEEE Transactions on Consumer Electronics*, 53(2):593–600, 2007. 1
- [2] M. Abdullah-Al-Wadud, M. H. Kabir, M. A. A. Dewan, and O. Chae. A dynamic histogram equalization for image contrast enhancement. *IEEE Transactions on Consumer Electronics*, 53(2), 2007. 1
- [3] T. Arici, S. Dikbas, and Y. Altunbasak. A histogram modification framework and its application for image contrast enhancement. *IEEE Transactions on image processing*, 18(9):1921–1935, 2009. 1
- [4] A. Beghdadi and A. Le Negrate. Contrast enhancement technique based on local detection of edges. *Computer Vision, Graphics, and Image Processing*, 46(2):162–174, 1989. 1
- [5] S.-H. Chang and H.-H. P. Wu. Improved measurement of camera response function and its performance evaluation. *Applied optics*, 53(1):82–89, 2014. 1
- [6] S.-D. Chen and A. R. Ramli. Contrast enhancement using recursive mean-separate histogram equalization for scalable brightness preservation. *IEEE Transactions on Consumer Electronics*, 49(4):1301–1309, 2003. 1

¹<https://github.com/baidut/OpenCE>.

- [7] S.-D. Chen and A. R. Ramli. Minimum mean brightness error bi-histogram equalization in contrast enhancement. *IEEE transactions on Consumer Electronics*, 49(4):1310–1319, 2003. [1](#)
- [8] D. Cheng, D. K. Prasad, and M. S. Brown. Illuminant estimation for color constancy: why spatial-domain methods work and the role of the color distribution. *JOSA A*, 31(5):1049–1058, 2014. [5](#)
- [9] D. Coltuc, P. Bolon, and J.-M. Chassery. Exact histogram specification. *IEEE Transactions on Image Processing*, 15(5):1143–1152, 2006. [1](#)
- [10] P. E. Debevec and J. Malik. Recovering high dynamic range radiance maps from photographs. In *ACM SIGGRAPH 2008 classes*, page 31. ACM, 2008. [2](#)
- [11] X. Dong, G. Wang, Y. Pang, W. Li, J. Wen, W. Meng, and Y. Lu. Fast efficient algorithm for enhancement of low lighting video. In *2011 IEEE International Conference on Multimedia and Expo*, pages 1–6. IEEE, 2011. [1](#), [5](#)
- [12] X. Fu, D. Zeng, Y. Huang, X.-P. Zhang, and X. Ding. A weighted variational model for simultaneous reflectance and illumination estimation. In *Proceedings of the IEEE Conference on Computer Vision and Pattern Recognition*, pages 2782–2790, 2016. [1](#)
- [13] R. Gonzalez and R. Woods. Digital image processing: Pearson prentice hall. *Upper Saddle River, NJ*, 2008. [1](#)
- [14] M. D. Grossberg and S. K. Nayar. What is the space of camera response functions? In *Computer Vision and Pattern Recognition, 2003. Proceedings. 2003 IEEE Computer Society Conference on*, volume 2, pages II–602. IEEE, 2003. [2](#)
- [15] M. D. Grossberg and S. K. Nayar. Modeling the space of camera response functions. *IEEE transactions on pattern analysis and machine intelligence*, 26(10):1272–1282, 2004. [2](#)
- [16] X. Guo, Y. Li, and H. Ling. Lime: Low-light image enhancement via illumination map estimation. *IEEE Transactions on Image Processing*, 26(2):982–993, 2017. [1](#), [4](#), [5](#), [6](#)
- [17] H. Ibrahim and N. S. P. Kong. Brightness preserving dynamic histogram equalization for image contrast enhancement. *IEEE Transactions on Consumer Electronics*, 53(4):1752–1758, 2007. [1](#)
- [18] A. K. Jain. *Fundamentals of digital image processing*. Prentice-Hall, Inc., 1989. [1](#)
- [19] L. Li, R. Wang, W. Wang, and W. Gao. A low-light image enhancement method for both denoising and contrast enlarging. In *Image Processing (ICIP), 2015 IEEE International Conference on*, pages 3730–3734. IEEE, 2015. [1](#)
- [20] S. Lynch, M. Drew, and G. Finlayson. Colour constancy from both sides of the shadow edge. In *Proceedings of the IEEE International Conference on Computer Vision Workshops*, pages 899–906, 2013. [5](#)
- [21] K. Ma, K. Zeng, and Z. Wang. Perceptual quality assessment for multi-exposure image fusion. *IEEE Transactions on Image Processing*, 24(11):3345–3356, 2015. [6](#)
- [22] S. Mann. Comparametric equations with practical applications in quantigraphic image processing. *IEEE transactions on image processing*, 9(8):1389–1406, 2000. [2](#), [3](#), [4](#)
- [23] T. Mitsunaga and S. K. Nayar. Radiometric self calibration. In *Computer Vision and Pattern Recognition, 1999. IEEE Computer Society Conference on.*, volume 1. IEEE, 1999. [2](#)
- [24] S. K. Nayar and T. Mitsunaga. High dynamic range imaging: Spatially varying pixel exposures. In *Computer Vision and Pattern Recognition, 2000. Proceedings. IEEE Conference on*, volume 1, pages 472–479. IEEE, 2000. [2](#)
- [25] T.-T. Ng, S.-F. Chang, and M.-P. Tsui. Using geometry invariants for camera response function estimation. In *2007 IEEE Conference on Computer Vision and Pattern Recognition*, pages 1–8. IEEE, 2007. [2](#)
- [26] E. Peli. Contrast in complex images. *JOSA A*, 7(10):2032–2040, 1990. [1](#)
- [27] A. B. Petro, C. Sbert, and J.-M. Morel. Multiscale retinex. *Image Processing On Line*, pages 71–88, 2014. [5](#)
- [28] A. M. Reza. Realization of the contrast limited adaptive histogram equalization (clahe) for real-time image enhancement. *Journal of VLSI signal processing systems for signal, image and video technology*, 38(1):35–44, 2004. [1](#)
- [29] D. Sen and S. K. Pal. Automatic exact histogram specification for contrast enhancement and visual system based quantitative evaluation. *IEEE Transactions on image processing*, 20(5):1211–1220, 2011. [1](#)
- [30] K. Sim, C. Tso, and Y. Tan. Recursive sub-image histogram equalization applied to gray scale images. *Pattern Recognition Letters*, 28(10):1209–1221, 2007. [1](#)
- [31] J. A. Stark. Adaptive image contrast enhancement using generalizations of histogram equalization. *IEEE Transactions on image processing*, 9(5):889–896, 2000. [1](#)
- [32] G. Thomas, D. Flores-Tapia, and S. Pistorius. Histogram specification: a fast and flexible method to process digital images. *IEEE Transactions on Instrumentation and Measurement*, 60(5):1565–1578, 2011. [1](#)
- [33] V. Vonikakis, I. Andreadis, and A. Gasteratos. Fast centre-surround contrast modification. *IET Image processing*, 2(1):19–34, 2008. [6](#)
- [34] V. Vonikakis, I. Andreadis, and A. Gasteratos. Fast centre-surround contrast modification. *IET Image Processing*, 2(1):19, 2008. [1](#)
- [35] C. Wang and Z. Ye. Brightness preserving histogram equalization with maximum entropy: a variational perspective. *IEEE Transactions on Consumer Electronics*, 51(4):1326–1334, 2005. [1](#)
- [36] L. Wang, L. Xiao, H. Liu, and Z. Wei. Variational bayesian method for retinex. *IEEE Transactions on Image Processing*, 23(8):3381–3396, 2014. [1](#)
- [37] L. Wang, L. Xiao, H. Liu, and Z. Wei. Variational bayesian method for retinex. *IEEE Transactions on Image Processing*, 23(8):3381–3396, aug 2014. [1](#)
- [38] S. Wang, J. Zheng, H.-M. Hu, and B. Li. Naturalness preserved enhancement algorithm for non-uniform illumination images. *IEEE Transactions on Image Processing*, 22(9):3538–3548, 2013. [1](#), [5](#), [6](#)
- [39] X. Wang and D. Zhang. An optimized tongue image color correction scheme. *IEEE Transactions on information technology in biomedicine*, 14(6):1355–1364, 2010. [5](#)